DESIGN AND WIND TUNNEL TESTING OF CAL POLY'S AMELIA 10 FOOT SPAN HYBRID WING-BODY LOW NOISE CESTOL AIRCRAFT

Kristina K. Jameson*, David D. Marshall*, Robert Ehrmann*, Eric Paciano*, Rory Golden*, and Dave Mason**
***California Polytechnic State University, San Luis Obispo, **PatersonLabs**

Keywords: *Powered-lift, Circulation Control, CFD database, NFAC*

Abstract

California Polytechnic Corporation, Georgia Tech Research Institute (GTRI), and DHC Engineering collaborated on a NASA NRA to develop and validate predictive capabilities for the design and performance of Cruise Efficient, Short Take-Off and Landing (CESTOL) subsonic aircraft. In addition, a large scale wind tunnel effort to validate predictive capabilities for aerodynamic performance and noise during takeoff and landing has been undertaken.

The model, Advanced Model for Extreme Lift and Improved Aeroacoustics (AMELIA), was designed as a 100 passenger, N+2 generation, regional, CESTOL airliner with hybrid blended wing-body with circulation control. The model design was focused on fuel-savings and noise goals set out by the NASA N+2 definition. The AMELIA is 1/13 scale with a 10 ft wing span. PatersonLabs was chosen to build AMELIA and The National Full-Scale Aerodynamic Complex (NFAC) 40 ft by 80 ft wind tunnel was chosen to perform the nine week long large scale wind tunnel test in the summer of 2011.

1 Introduction

With the very recent advent of NASA's Environmentally Responsible Aviation Project (ERA)[1], dedicated to designing aircraft that will reduce the impact of aviation on the environment, there is a need for research and development of methodologies to minimize fuel burn, emission, and a reduction in community noise produced by regional airlines. ERA is specifically concentrating in the areas of airframe technology, propulsion technology, and vehicle systems integration all in the time frame for the aircraft to be at a Technology Readiness Level (TRL) of 4-6 by the year of 2020 (deemed N+2). The proceeding project looking into similar issues was led by NASA's Subsonic Fixed Wing Project and focused on conducting research to improve prediction methods and technologies that will produce lower noise, lower emissions, and higher performing subsonic aircraft for the Next Generation Air Transportation System.

The work provided in this investigation was an NRA funded by Subsonic Fixed Wing Project starting in 2007 with a specific goal of conducting a large scale wind tunnel test along with the development of new and improved predictive codes for the advanced powered-lift concepts incorporated into the wind tunnel model in conjunction with the verification of these codes with the experimental data obtained during the wind tunnel test. Powered-lift concepts investigated are Circulation Control (CC) wing in conjunction with over the wing mounted engines to entrain the exhaust and further increase the lift generated by CC technologies alone.

There are a number of papers in the past few years presenting computational studies of CC technologies. Most of them have focus on 2D studies[2-11] While there are a number of excellent 2D experimental datasets available for such CFD validation[12-15], the same is not

true for 3D experimental data[16]. This effort aims to address this short fall by creating a comprehensive and relevant 3D database for current and future 3D simulations. Experimental measurements included in the database will include forces and moments, surface pressure distributions, local skin friction, boundary and shear layer velocity profiles, far-field acoustic data and noise signatures from turbofan propulsion simulators. This paper focuses on designing and developing a model with NASA's N+2 goals for less environmental impact as well as the fabrication of a 10 foot span wind tunnel model to be used to create the 3D validation database for numerical simulations. The resulting design is the Advanced Model for Extreme Lift and Improved Aeroacoustics (AMELIA) and is the subject of the rest of this paper.

2 Advanced Model for Extreme Lift and Improved Aeroacoustics (AMELIA)

2.1 Summary of NASA's N+2 Design Goals

NASA is committed to identify solutions that meet improvements for noise, emissions, and energy usage (fuel burn). They have classified the N+2 design metrics as a 40% reduction in fuel consumption, progress towards -42 dB lower noise levels, a 70% decrease in emissions, and a 50% reduction in field length performance over current generation aircrafts. Theoretically the aircraft should reach a Technology Readiness Level (TRL) of 4-6 by the year 2020.

Dave Hall at DHC Engineering did the conceptual design of four separate configurations to address the N+2 goals with a down selection to one favorable configuration. This yielded the Advanced Model for Extreme Lift and Improved Aeroacoustics (AMELIA).

2.2 Conceptual Designs Considered

Four CESTOL configurations were developed for consideration for the large scale wind tunnel test. The first concept, Configuration 1, has a more conventional appearance with a high aspect ratio wing, a tee-tail, and twin engines configured over the wing, as can be seen in Fig. 1. The trailing edge wing surface aft of the engine is designed for turning the flow to create powered-lift.

Fig. 1. Conceptual design of Configuration 1 consisting of a high aspect ratio wing, a tee-tail, and twin engines configured over the wing.

The second concept, Configuration 2, is a hybrid blended-wing-body. The design utilizes circulation control at the leading and trailing edges of the wing. This configuration utilizes over the wing engine locations for noise shielding and engine exhaust entrainment purposes. A structural rudder and V-tail were also employed in this design. Configuration 2 is shown in Fig. 2.

Fig. 2. Conceptual design of Configuration 2 consisting of circulation control wings and over the wing engine mounting for enhanced powered lift.

The third aircraft configuration was inspired by the extensive research now underway to develop a true Blended-Wing-Body aircraft, BWB, by the Boeing Company[17]. This aircraft concept is a significant departure from the first two aircraft designs. The turbofan engines are embedded within the very thick wing root as the wing blends into the fuselage, as shown in Fig. 3. The exhaust discharges

through a high aspect ratio 2-D nozzle at the trailing edge of the vehicle. The intent is not only to produce thrust through this nozzle throughout the flight but to create increased flow circulation around the aircraft generating additional lift.

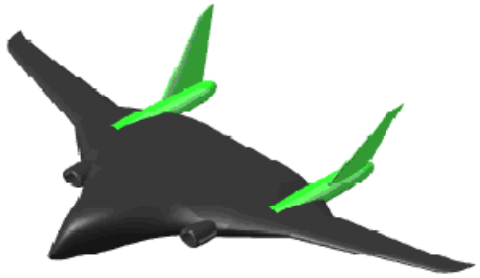

Fig.3 Conceptual design of Configuration 3 consisting of a blended wing body and embeded engines.

The final design, seen in Fig. 4, is termed the Diamond-Wing-Body (DWB). It may be thought of as a Joined-Wing with a vertical structural member joining the fore and aft wings at the outer span points. The intent is to improve local air flow and mitigate shock formation at high subsonic Mach numbers. These vertical members are more like wingtip sails than winglets and act structurally as struts. The forward wing sweeps aft and the aft wing sweeps forward forming a diamond planform shape in the top view. Both wings have a high aspect ratio. The chosen propulsion system is a medium-sized geared turbofan engine mounted in a channel wing.

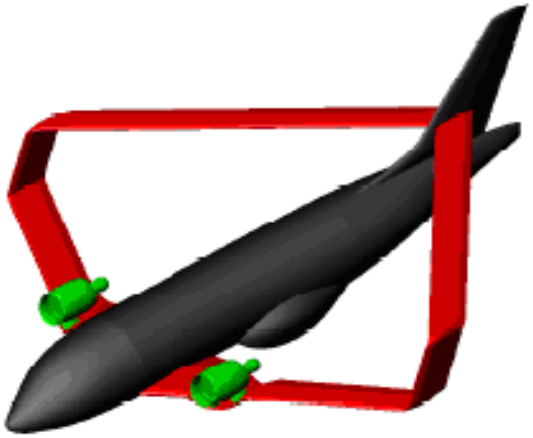

Fig. 4. Conceptual design of Configuration 4 consisting of high aspect ratio diamond-wing design with channel wing mounted engines.

2.3 Configuration 2 Becomes AMELIA

After close consideration of each design, it was apparent that Configuration 1 was too conventional to be an N+2 design. Configuration 4 on the other hand was too advanced to be considered within an N+2 time frame. A large scale wind tunnel test, being conducted by a competing NRA utilized a test model that was similar to Configuration 3 in that it was a blended wing body with circulation control wings[18]. Configuration 2 was considered to be at the appropriate level for the N+2 time frame. Further investigations into this design also showed that a 10' span model based on Configuration 2 would not exceed the load limits of all our perspective test locations. After consulting all involved in this project, it was decided that Configuration 2—the hybrid blended wing body—was best suited for the AMELIA test. Figure 5 shows a rendering of Configuration 2 in flight after many design iterations.

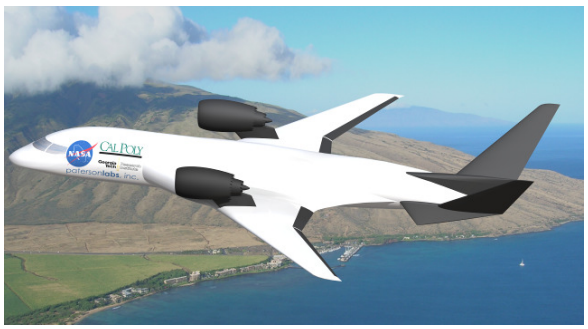

Fig. 5. Rendered image of Configuration 2 - the Hybrid Blended Wing Body in flight.

2.4 AMELIA Design Features

In order to utilize the Configuration 2 geometry in a large scale wind tunnel test setting, many design modifications were needed. The most significant alteration to the geometry came in the mounting system of the wind tunnel model. A sting was chosen as the ideal method to measure aerodynamic forces and moments, mainly for its ability to take measurements non-intrusively. Direct mounting of the model to the sting through the aft end raised concerns with disturbing the flow around the beaver tail. An underbody mount was designed to provide an attachment location with

minimal flow disturbance. The mount is faired with a clamshell blade that extends vertically from the sting tip. For purposes discussed in subsequent sections the model will be inverted for a portion of the test, as a result the negative angle of attack limit of the sting needed to be extended. The blade mount also serves to extend this negative limit. Figure 6 shows a three view drawing of the model mounted to the blade attachment with empennage removed and relevant dimensions shown. The tail empennage is not shown in the three-view because it will not be attached to the model during the majority of the testing, due to the fact that the main focus of the testing is on aeroacoustic and aerodynamic measurements. The strakes, structural rudder and V-tail seen in the previous figure were manufactured in order to supplement subsequent research and testing. These surfaces attach to the model via off blocks.

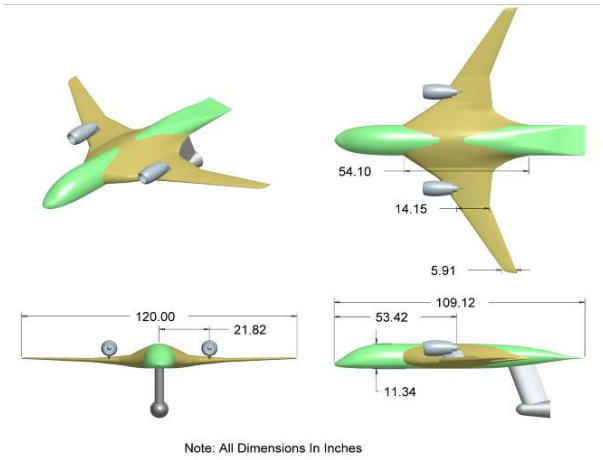

Fig. 6 Three-view drawing of AMELIA with sting-blade attachment with the tail surfaces removed.

The selected configuration utilizes an optimized supercritical airfoil [please see Ref. 19-20 for further details] with a dual radius flap at the trailing edge[Please see Ref. 21 for further details]. In order to minimize cost and complexity dual radius flaps of 0º, 30º, 60º and 90º deflections were proposed to be manufactured, as opposed to a mechanical flap where deflection can be varied. The 90º flap deflection was later changed to 80º due to issues with the manufacturing of the flap. The flaps of the Configuration 2 design were also modified to be a single continuous flap for each wing, in order to reduce the amount of flow disturbance from discontinuities of the flap surface. A cut away view of the model, with the 80° flap, is shown in Fig. 7.

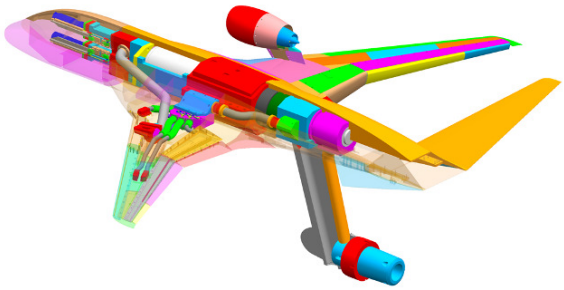

Fig 7. Cut away of the AMELIA showing the internal structure along with the sting-blade attachment and tail empennage on the manufacturing model.

The piping seen in Fig. 7 exiting the blade supplies the necessary high and low pressure air to the model. The larger blue pipe supplies the high pressure air required to power the Turbine Propulsion Simulator (TPS) units, while the smaller amber pipe provides the low pressure air necessary for the circulation control slots at the leading and trailing edges. The details of the piping systems will be discussed in subsequent sections.

As shown in Configuration 2 the TPS units will be mounted over the wing, however two mounting heights will be tested in order to study the effects of engine height on entrainment of exhaust in the circulation control flow. Height adjustments will be completed using faired structural pylons of two different heights [see Ref. 22-23 for the optimal engine height location]. These pylons also act as pressure vessels within which the high pressure air is fed to the TPS units.

2.5 AMELIA Instrumentation

As a CFD validation experiment it's imperative that the model be highly instrumented in order to capture the maximum amount of data. Almost all instrumentation placement occurs on the left wing and was chosen based on preliminary CFD results. Figure 8 is a half-span schematic of the model illustrating the relative placement of the

pressure ports and unsteady pressure transducers. The model is instrumented with 280 static pressure ports in five chordwise groups and one spanwise group (highlighted in red in Fig. 8). Five static pressure ports are located on the right wing in order to verify symmetry in the pressure distribution.

Eight unsteady pressure Kulites exist on the model (shown as blue circles in Fig. 8). As aeroacoustics is one of the main focuses of the large scale test, five Kulites are located in line with the engine assembly. The remaining three Kulites are located at the estimated passengers head level, on the wing blend to gain a better understanding of the implications of over the wing mounted engines and passenger comfort level. Six stationary microphones will be placed underneath model approximately 5 ft above the tunnel floor (in order to be sufficiently out of the boundary layer) to measure far-field noise generated by the powered-lift design. A 70 element stationary microphone array will also be placed directly underneath the wing below one of the propulsion simulators to determine the noise signature associated with TPS unit.

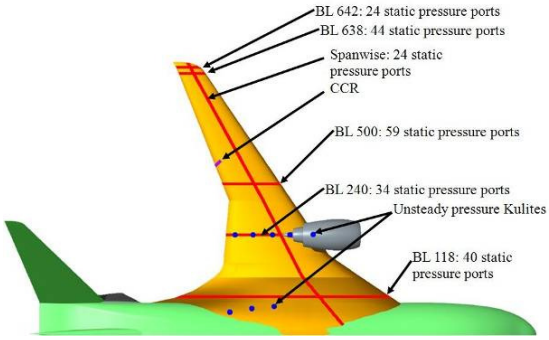

Fig. 8. Half-span schematic of AMELIA illustrating the relative location of the pressure ports and unsteady pressure transducers on the left half of the model.

In order to monitor the health of the TPS units, each unit is instrumented with seven rakes, each consisting of 4 total pressure probes and a thermocouple. The design and amount of these rakes were based on discussions with engineers from industry who have previous experience with TPS units.

Each of the circulation control plenums is instrumented with 3 total pressure probes (the plenums can be seen in Fig. 7), while a cross correlation rake measures boundary layer interactions at the plenum exit or slot. Further discussion of the design and theory behind the cross correlation rake can be found in Section 5.

The majority of the right wing is free of instrumentation in order for the local shear stress measurements to be obtained. In order to take high fidelity measurements, the surface must be of number 2 finish (mirror like) or better. For this reason the model will be painted with a black Imron coating.[24] Further discussion of the requirements of the technique will be discussed in Section 4.

2.6 Internal Design of AMELIA

The model is supplied using two separate air systems for the propulsion simulators and the blown slots. Figure 9 shows a complete cut-away schematic of the model showing the internal piping for both the high and low pressure systems.

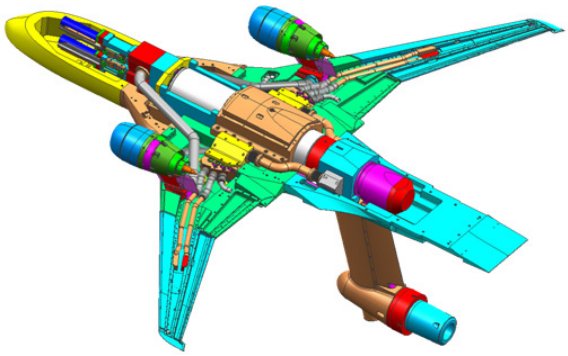

Fig. 9. A complete cut-away schematic of AMELIA showing the 8 in flow thru balance and the internal piping for both the high and low pressure systems.

The high pressure air system (600 psi maximum determined by the limits of the flow thru balance) is supplied thru the NASA provided sting into the fabricated strut. The air passes up the strut and through the 8in flow thru balance. On the front of the balance is a flow control system that controls the air flow to the left and right hand TPS units. The airflow is controlled using conical plugs that can be remotely controlled while the tunnel is running. The conical plugs are driven using MMP 24vdc gear motors, and use linear potentiometers for position feedback. The plugs can be positioned

to provide from 0-100% mass flow. The TPS units are supplied through stainless steel pipes that attach to wing mounted pylons that feed the TPS units. Figure 10 shows the complete piping and mass flow control plenum for the high pressure air system along with the sting-blade attachment.

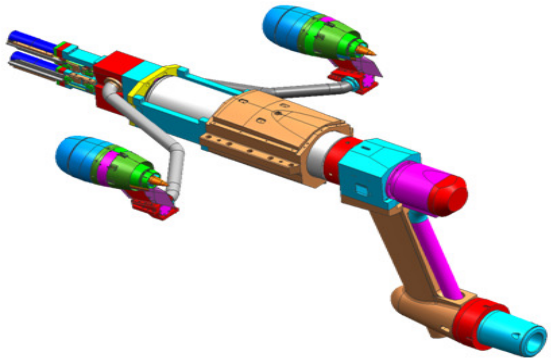

Fig. 10. A schematic of the high pressure air system internal to AMELIA.

The low pressure system (approximately 100 psi) will be used to supply the air to the plenums that feed the slots at the leading and trialing edges for the circulation control wing. The low pressure system is controlled using 24vdc gear motors, with rotary pots for feedback. The flow to each plenum can be controlled individually from the control room. To isolate and minimize adverse effects on the balance the low pressure plenum is fed by a pipe that has bellows at each end of the pipe, as shown in Fig. 11.

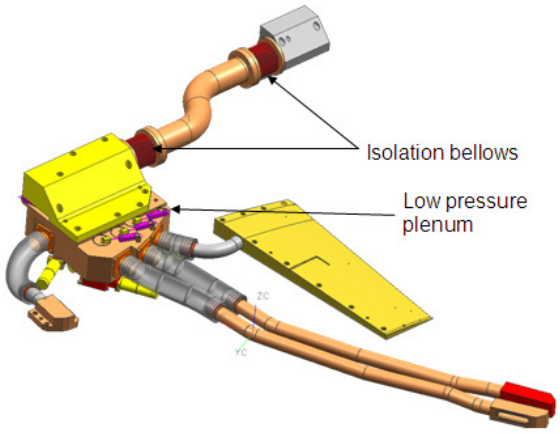

Fig. 11. An internal schematic of the piping for the low pressure system along with the bellows for system isolation downstream of the sting-blade attachment.

3 Large Scale Wind Tunnel Test - NFAC

3.1 Wind Tunnel Test Facility

The National Full-Scale Aerodynamic Complex (NFAC) 40 ft by 80 ft wind tunnel was chosen to perform the nine week long large scale wind tunnel test. The NFAC offered several benefits over other large wind tunnels across the United States, with the most significant being: the 10 foot model could be mounted on a sting which allows for cleaner measurements of the produced aerodynamic forces and moments, the tunnel could supply the high pressure air at the mass flow rate necessary to operate the CCW slots and the turbofan simulators, the tunnel is large enough such that the downwash created by the CCW wings would not impinge on the floor of the tunnel thus creating cleaner far-field acoustic measurements, the tunnel was acoustically treated such that aerodynamic and acoustic measurements could be performed simultaneously, and the NFAC's cost and schedule fit within Cal Poly's time frame and budget. Figure 12 shows a scale schematic of the model inverted on the sting in the 40 ft by 80 ft NFAC wind tunnel with the associated acoustic measurement devices mounted on the tunnel floor relative to the wind tunnel model placed in the center of the tunnel. Figure 13 shows the relative scale of AMELIA in the NFAC.

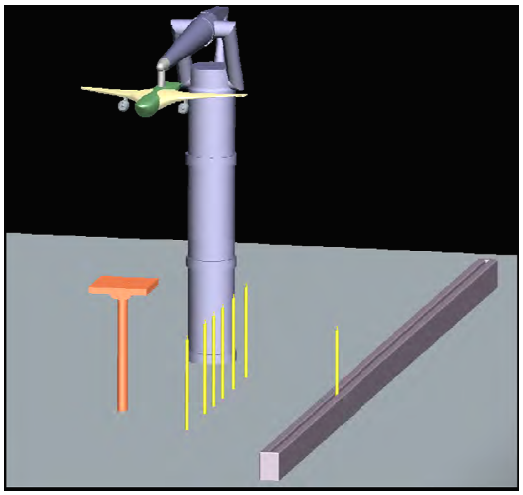

Fig. 12. A schematic of AMELIA mounted and inverted on the sting in the NFAC along with the far-field stationary microphones and the stationary acoustic array.

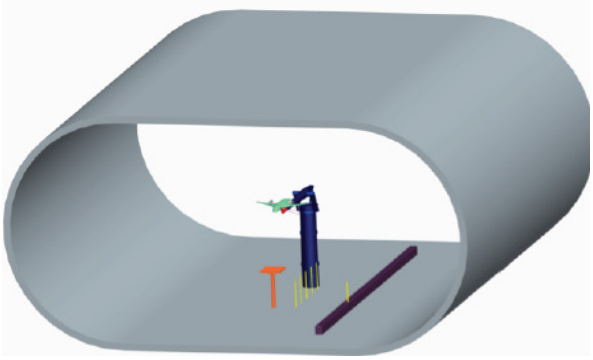

Fig. 13. Isometric view of AMELIA mounted on the sting in the NFAC.

3.2 AMELIA Test Matrix

The proposed text matrix for the model includes calibrations while mounted on the sting balance of both model and acoustic instrumentation, static tests of all blown features on the model, a Reynolds number sweep, a dynamic pressure sweep, a turbofan simulator sweep, and a CCW sweep.

After the completion of the preliminary sweeps, eight to ten critical tests points will be identified from the experimental test data obtained. During the critical tests points all experimental instrumentation will be utilized. Acoustically, the far-field measurements along with a traversing 30 degree sideline measurements will be made. Also the 70 element stationary array placed under one of the turbofan simulators will be utilized to characterize the noise signature beneath the wing. The aerodynamic forces, moments, static pressure measurements, and unsteady pressure measurements will simultaneously be conducted. Then the model will be inverted and the same critical test points will be repeated. Inverting the model offers several advantages in obtaining experimental measurements. The oil interferometry requires less lighting in the large wind tunnel and high power lights can be shown directly on the reflective surface. The 70 element stationary array can be utilized to identify any hot spots created by the TPS units. The cross correlation rake will also be utilized while the model is inverted.

Once the critical test points have been completed, the model will be returned to right side up and alpha (up to +20 to -5 degrees) and beta (+20 to -20 degrees) sweeps will be conducted at three different tunnels speeds. The majority of the tests will be conducted at lower tunnel speeds in order to correctly match the necessary design thrust coefficients (limited by the TPS thrust output). Only far-field acoustic measurements, aerodynamic forces and moments, and static pressure measurements will be conducted for this portion of the test allowing a significant number of test points to be investigated to create the database for current and future CFD validation efforts.

4 Oil Interferometry

The Fringe-Image Skin Friction (FISF) technique, also known as oil interferometry, was chosen for the large scale wind tunnel test to measure local skin friction because both magnitude and direction can be determined from a single image. The FISF technique has the advantage of maturity and reliability which becomes significant due to the difficulties of obtaining measurements in the NFAC due to its sheer size and the amount of time between tunnel shut down and the point where photographs of the model can be obtained.

4.1 FISF Technique

The FISF technique was developed by Monson et al.[25] The theory behind the technique is that a single relationship can relate the thickness of the oil drop at a single location to the skin friction magnitude and direction. The oil thickness is measured via photographic interferometry. Data reduction is completed with CXWIN4GG, a PC application developed by Zilliac.[26]

The FISF technique has a few key steps in its process to obtain the crucial photographs necessary to determine surface skin friction. The process is as follows: A drop of silicone oil of known viscosity is placed on the model surface. Once the oil is applied to the surface, the air flow begins, causing the oil to spread and thin. The air continues to flow for a given time, continually thinning the oil. When sufficient time has elapsed (2-20 minutes, depending on oil viscosity), the air flow is turned off. A quasi-monochromatic light source is then indirectly applied to the surface by use of a large diffuse

reflector. Light is reflected from the surface of the model and oil. Two specific light rays are reflected and separated by the thickness of the oil, shown in Fig. 14. Once the oil has thinned, the oil height linearly varies where constructive and destructive interference occurs, causing light and dark fringes on the oil surface. Skin friction is proportional to the spacing distance, Δs, on the fringes which is directly related to the thickness of the oil. The relationship for skin friction is as follows:

$$C_f = \frac{\tau_W}{q_\infty} = \frac{2 n_o \mu_o \Delta s}{q_\infty \lambda t} \cos(\theta_r) \quad (1)$$

where C_f is the skin friction coefficient, τ_w is the wall shear stress, q_∞ is the freestream dynamic pressure, n_o is the oil index of refraction, μ_o is the oil viscosity, λ is the wavelength of the light source, t is the duration of time the oil flow was exposed to air flow, and θ_r is the light refraction angle through the air-oil interface. Eq. 1 holds for zero pressure gradient and shear stress gradients. Further details on the oil flow technique and the theory behind it is covered by Naughton and Sheplak.[27]

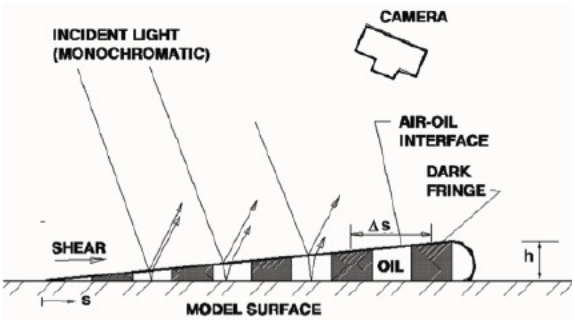

Fig. 14. A schematic of the basic FISF setup highlighting the oil flow and fringe pattern on a droplet of oil[27].

4.2 Application of FISF to AMELIA

In order to successfully apply the FISF technique, the fringes on a model need to be clearly visible. Fringe visibility is based upon the surface finish of the model. An ideal surface is extremely smooth with consistent and durable optical properties. Based on a study by Zilliac[28] the best fringes appeared on high flint content SF11 glass manufactured by Schott Glass of Germany, which is an impractical material for a wind tunnel model. A practical surface finish for a model would be mirror like, which can be achieved by nickel plating the model surface. Acceptable substitutes have been made utilizing polished stainless steel or black Mylar sheets applied to the model surface. Black Mylar sheets offer the most cost effective solution for oil flow testing. However, at higher speeds and long run times Mylar would begin to peal along the edges, ruining any data downstream. The continual Mylar reapplication to the model would prove time consuming and impractical due the model height in the NFAC for the AMELIA test. Mylar is also difficult to apply to a 3D surface, usually resulting in small wrinkles in the Mylar distorting the skin friction measurements. Polished stainless steel and nickel plating have the durability that Mylar lacks. Another alternative to nickel plated aluminum is aluminum painted with black Imron. Difficulties arose in the capability of plating the fuselage of AMELA due to its sheer size. For these reasons, the entire model will be painted with Imron, also allowing future experiments with AMELIA to investigate other regions besides the wing.

In order to properly view the fringes, a monochromatic light source must be reflected off a diffuse reflector. In large wind tunnel applications, the tunnel walls have been used as the reflector.[29] Unfortunately, the NFAC tunnels walls are composed of a matte metal mesh covering a deep, perforated acoustic liner, rendering the walls unable to sufficiently light the tunnel. The next option is to build a reflector which encompasses the portion of interest on the model. A small hole would be cut in the reflector allowing a camera to capture the fringe spacings; a setup such as this is shown in Fig. 4. AMELIA has a highly curved blended wing which causes additional difficulty in the image processing. Due to the models highly polished and curved surfaces, the camera will see reflections from a large area of the wind tunnel. Therefore, if the wind tunnel is being used as the diffuse reflector, large areas of the tunnel need to be white. Since this would be costly in the NFAC, it is necessary to use a curved diffuse reflector. This will ensure the model is uniformly lit allowing for accurate fringe

spacing identification and does so with fewer lights. The type of diffuse reflector used on the wing blend is also shown in Fig. 15.

The angle at which the light enters the camera can greatly affect the skin friction measurement, especially at large angles such as leading edges or the blended wing portion of the model. Zilliacs CXWIN4GG software utilizes single camera photogrammetry to determine the angle of the light reflecting off the oil on the surface of the wind tunnel model. This is made possible by using fiducial marks over the model surface. The camera captures an image encompassing the entire wing with several fringes over the wing surface. Within that image are multiple fiducial marks with known locations on the model coordinate system. Zilliacs software completes the photogrammetry by matching the known fiducial marks locations (both a pixel x-y coordinate system as well as the model coordinate) to a given set of model points. This allows the software to calculate the light incident angle at any visible point on the model.

Due of the size of the NFAC, a special procedure has been devised to ensure accurate fringe production. Normally the tunnel transients are short, resulting in little error from the startup and shutdowns. However, the NFAC requires a minimum of 5 minutes to startup and shutdown which can introduce unacceptable error into the skin friction measurements if the incorrect viscosity of oil is chosen for the test. In order to ensure recording accurate fringes, the model will be at a high angle of attack during the tunnel startup allowing separated flow (low to no shear) over the wing. Once the tunnel freestream has been reached, the model will be positioned to the angle of attack of interest. At this point, slot blowing and the turbine simulators will be started as well. The model will remain at this test condition for a minimum of 20 minutes. Once the oil is sufficiently spread, the slot blowing, turbine simulator, and tunnel freestream will be turned off, while the model is once again pitched upward to cause separation over the wing allowing the fringes to be unaffected by the shutdown procedure. Once the flow has stopped, the diffuse reflector and camera will be brought into the tunnel. The model will be inverted for the skin friction measurements, allowing for optical access to the suction side of the airfoil without having to be physically placed above the model. A diffuse reflector will be held up to the model, lighting it, while a second person will capture the fringe spacings in two images. This process is time consuming, but worthwhile to ensure quality data for CFD validations to be made against. For this reason, only eight to ten key test conditions will be investigated with oil interferometry for CFD validation. Please refer to Ref. 30 for further investigation of the FISF technique for the preparation of the AMELIA test.

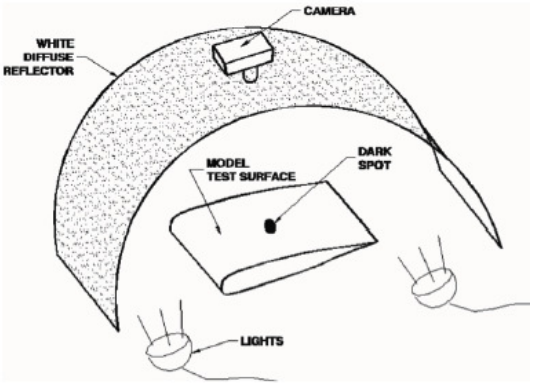

Fig. 15. The FISF solution used for the wing blend. The dark spot is due to no light being reflected by the camera lens.

5 Boundary and Shear Layer Velocity Profiles with a Micro Flow Measurement Device

5.1 Application of FISF to AMELIA

In 2001, NASA Glenn developed a thermocouple boundary layer rake which has the capability to measure 0.0025 inches from the surface, four times closer than any state of the art measurement before.[31] This was achieved with the device shown in Fig. 16. This device is constructed with a base made out of aluminum, a constant thickness strut which protrudes from the base, and the necessary electrical wires corresponding to the number of thermocouples present for a given design. The strut is made of quartz, chosen for its insulative

and low thermal expansion properties. From the base to the top of the strut, there are several pairs of thermocouples. The device functions based on the theory that for a given height above the base, the velocity is equal to the velocity of the flow as if there were no strut present. It should be noted that no horseshoe vortices were found to be shed at the intersection of the strut and base in NASA Glenn's testing of the thermocouple rake.[32]

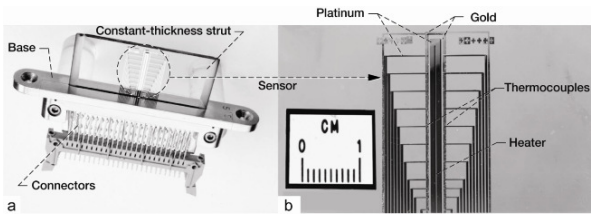

Fig. 16. Photographs of a thermocouple boundary layer rake, a) shows the base and electrical connections and b) detail of platinum and gold films.[32]

At the center of the strut, there is a platinum loop which is heated to a temperature above ambient. As air flows over the loop, the air downstream is heated. The voltage difference between the upstream and downstream thermocouples is then related to known velocity values obtained from a total pressure rake setup next to the thermocouple rake at exactly the same axial position. A calibration curve can be developed from this data. This calibration procedure is needed for every Reynolds number intended for testing.

Upon further discussions with Gustave Fralick, one of the thermocouple rake's designers, a Cross Correlation Rake (CCR) was suggested for use since an in situ calibration process would prove difficult in the anticipated application. The CCR contains a conductive platinum loop located at the center of the substrate. This loop is heated to a temperature above the ambient conditions. Instantaneous voltage differences on the loop's leading edge and trailing edge are measured by voltage taps along the loop. The voltage fluctuations in the loop are caused by fluctuations in the local resistance. The resistance relates to the loop temperature, which relates directly with velocity at that location.[33] Utilizing a cross correlation script from MATLAB[34], the time between voltage fluctuations on the upstream and downstream voltage taps can be calculated. Since the distance between the upstream and downstream edges of the loop is known, the flow velocity can be calculated.

5.2 Application of CCR to AMELIA

The AMELIA model has both leading and trailing edge blowing in order to vastly increase the lift. Part of the validation effort will be to acquire velocity profiles above the flap. The CCR will be implemented as shown in Fig. 17 in order to achieve this. This region is of particular interest because of the jet's boundary layer as well as the shear layer above the jet. The design, construction, and validation of the CCR at subsonic speeds will be achieved [please see Ref. 35 for further detail on the design and construction of the CCR]. In addition, transonic speeds may be tested to demonstrate the CCR readiness on AMELIA. The substrate was constructed at Cal Poly, with the platinum applied to the substrate at NASA Glenn. The CCR will first be applied to a flat plate for validation purposes, then a trailing edge of an airfoil.

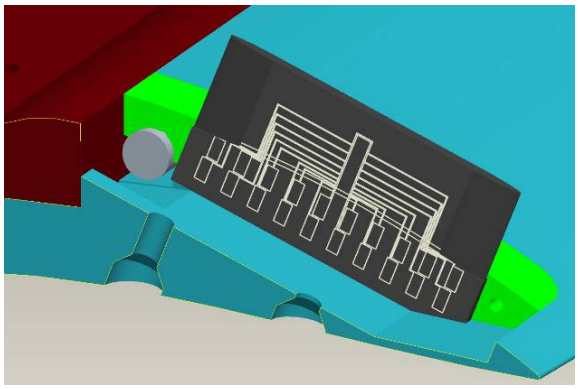

Fig. 17. A rendering of the Cross Correlation Rake applied to the AMELIA flap where the airfoil section is shown as in light blue and the mounting apparatus is shown in lime green.

The CCR designed for the AMELIA test is composed of a quartz substrate, platinum heating loop, and platinum voltage taps, as shown in the photograph in Fig. 18. The CCR was sized based on the AMELIA flap and was sized to 1.1 x 0.55 inches and 0.043 inches thick. It needed to be as large as possible

without being too near to the slot or trailing edge. The resulting length was 1.00 inch. The height was based upon the desired height above the flap to measure velocity profiles. This height was determined to be 0.12 inches. The total height of the rake is 0.040 inches, with the top half above the flap and the remaining lower half below the flap. Quartz microscope slides from Ted Pella, Inc. were utilized as the substrate. Microscope slides were only sold at a thickness of 1.0 mm. Figure 19 shows a completed CCR in the flat plate mounting device with only the exposed surface and the associated wires for the rake.

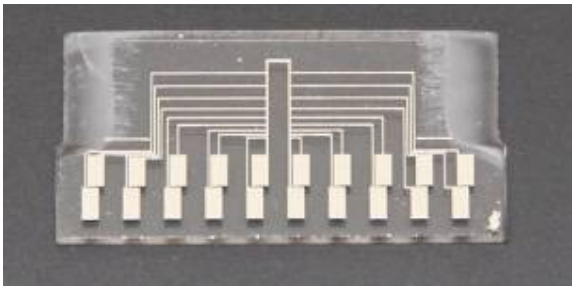

Fig. 18. Photograph of the Cross Correlation Rake of the first batch of rakes delivered to Cal Poly.

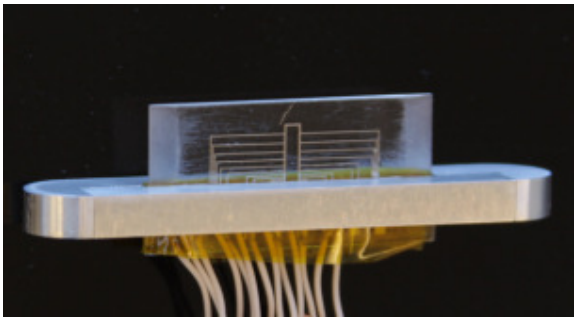

Fig. 19. Photograph of the completed Cross Correlation Rake mounted in the flat plate apparatus.

6 Conclusions

Cal Poly and GTRI researchers have completed a design for a large scale wind tunnel model in compliance of NASAs N+2 design goals. PatersonLabs has started fabrication of the model and at the time this paper was completed AMELIA was nearly 90% complete. The model has a projected delivery date of late September of 2010. Finally, large scale wind tunnel test activities are planned for the NFAC starting in the summer of 2011. These results will provide powered-lift and acoustic validation data for current and future 3D modeling efforts.

6 Acknowledgements

The authors would like to acknowledge the NASA Research Announcement award under Contract i#NNL07AA55C, with technical monitors Craig Hange and Clif Horne, who provided funding for this work. The authors wish to thank the Ames Research Center's Fluid Mechanics Lab, in particular, Gregory Zilliac and David Driver for the assistance in applying the FISF technique to AMELIA. The authors would also like to thank NASA Glenn, especially Gustave Fralick for his time and assistance.

References

[1] - Collier F. Overview of NASA's environmentally responsible aviation (ERA) project. 2009 Fundamental Aeronautics Conference, Atlanta GA, oral presentation, 2009.

[2] - Madugundi D, Nagib H and Kiedaisch J. Evaluation of turbulence models through prediction of separated flows with and without flow control and circulation effects. *46th AIAA Aerospace Sciences Meeting and Exhibit*, AIAA, Reno NV, AIAA-2008-0567, 2008.

[3] - McGowan G and Gopalarathnam A. Computational study of circulation control airfoil using FLUENT. *Applications of Circulation Control Technology*, edited by R. D. Joslin and G. S. Jones, Vol. 214 of Progress in Astronautics and Aeronautics, chap. 21, American Institute of Aeronautics and Astronautics, Inc., pp. 539-554, 2006.

[4] - McGowan G, Gopalarathnam A, Xiao X, and Hassan H A. Role of turbulence modeling in flow prediction of circulation control airfoils. *Applications of Circulation Control Technology,* edited by R. D. Joslin and G. S. Jones, Vol. 214 of Progress in Astronautics and Aeronautics, chap. 19, American Institute of Aeronautics and Astronautics, Inc., pp. 499-510, 2006.

[5] - Liu, Y., Sankar, L. N., Englar, R. J., Ahuja, K. K., and Gaeta, R. J. Computational evaluation of steady and pulsed set effects on a circulation control airfoil. *Applications of Circulation Control Technology*, edited by R. D. Joslin and G. S. Jones, Vol. 214 of Progress in Astronautics and Aeronautics, chap. 22, American Institute of Aeronautics and Astronautics, Inc., pp. 557-577, 2006.

[6] Chang III P A, Slomski J, Marino,T, Ebert M P, and Abramson J. Full Reynolds-stress modeling of circulation control airfoil. *Applications of Circulation Control Technology*, edited by R. D. Joslin and G. S. Jones, Vol. 214 of Progress in Astronautics and Aeronautics, chap. 17, American Institute of Aeronautics and Astronautics, Inc., pp. 445-466, 2006.

[7] Paterson E G and Baker W J. RANS and detached-eddy simulation of the NCCR airfoil. *Applications of Circulation Control Technology*, edited by R. D. Joslin and G. S. Jones, Vol. 214 of Progress in Astronautics and Aeronautics, chap. 16, American Institute of Aeronautics and Astronautics, Inc., pp. 421-444, 2006.

[8] Baker W J and Paterson E G. Simulation of steady circulation control for the general aviation circulation control (GACC) Wing. *Applications of Circulation Control Technology*, edited by R. D. Joslin and G. S. Jones, Vol. 214 of Progress in Astronautics and Aeronautics, chap. 20, American Institute of Aeronautics and Astronautics, Inc., pp. 513-537, 2006.

[9] Sahu J. Time-accurate simulations of synthetic jet-based flow control for a spinning projectile. *Applications of Circulation Control Technology*, edited by R. D. Joslin and G. S. Jones, Vol. 214 of Progress in Astronautics and Aeronautics, chap. 23, American Institute of Aeronautics and Astronautics, Inc., pp. 579-596, 2006.

[10] Zha G C and Paxton C D. Novel flow control method for airfoil performance enhancement using co-flow jet. *Applications of Circulation Control Technology*, edited by R. D. Joslin and G. S. Jones, Vol. 214 of Progress in Astronautics and Aeronautics, chap. 10, American Institute of Aeronautics and Astronautics, Inc., pp. 293-314, 2006.

[11] McGowan G, Rumsey C. L, Swanson R C, and Hassan H A. A three-dimensional computational study of a circulation control wing. *3rd AIAA Flow Control Conference*, AIAA, San Francisco CA, AIAA-2006-3677, 2006.

[12] Owen F K. Measurement and analysis of circulation control airfoils. *Applications of Circulation Control Technology*, edited by R. D. Joslin and G. S. Jones, Vol. 214 of Progress in Astronautics and Aeronautics, chap. 4, American Institute of Aeronautics and Astronautics, Inc., pp. 105-112, 2006.

[13] Cerchie D, Halfon E, Hammerich A, Han G, Taubert L, Trouve L, Varghese P, and Wygnanshi I. Some circulation and separation control experiments. *Applications of Circulation Control Technology*, edited by R. D. Joslin and G. S. Jones, Vol. 214 of Progress in Astronautics and Aeronautics, chap. 5, American Institute of Aeronautics and Astronautics, Inc., pp. 113-166, 2006.

[14] Munro S E, Ahuja K K, and Englar R J. Noise reduction through circulation control. *Applications of Circulation Control Technology*, edited by R. D. Joslin and G. S. Jones, Vol. 214 of Progress in Astronautics and Aeronautics, chap. 6, American Institute of Aeronautics and Astronautics, Inc., pp. 167-190, 2006.

[15] Jones G S. Pneumatic Flap Performance for a two-dimensional circulation control airfoil. *Applications of Circulation Control Technology*, edited by R. D. Joslin and G. S. Jones, Vol. 214 of Progress in Astronautics and Aeronautics, chap. 7, American Institute of Aeronautics and Astronautics, Inc., pp. 191-244, 2006.

[16] Englar R J. Experimental Development and evaluation of pneumatic powered-lift super-STOL aircraft. *Applications of Circulation Control Technology*, edited by R. D. Joslin and G. S. Jones, Vol. 214 of Progress in Astronautics and Aeronautics, chap. 7, American Institute of Aeronautics and Astronautics, Inc., pp. 191-244, 2006.

[17] Warwick G. Boeing works with airlines on commercial blended wing body freighter. Flight International, 2007.

[18] Collier F, Zavala E, and Huff D. Fundamental aeronautics program, subsonic fixed wing reference guide. NASA.

[19] Lane K A and Marshall D D. A surface parameterization method for airfoil optimization and high lift 2D geometries utilizing the CST methodology. *47th AIAA Aerospace Sciences Meeting and Exhibit*, AIAA, Orlando FL, AIAA-2009-1461, 2009.

[20] Lane K A and Marshall D D. Inverse airfoil design utilizing CST parameterization. *48th AIAA Aerospace Sciences Meeting and Exhibit*, AIAA, Orlando FL, AIAA-2010-1228, 2010.

[21] Golden R and Marshall D D. Design and performance of circulation control flap systems," *48th AIAA Aerospace Sciences Meeting and Exhibit*, AIAA, Orlando FL, AIAA 2010-1053, 2010.

[22] Englar R J, Gaeta R J, Lee W J and Leone V. Development of pneumatic over-the-wing powered-lift technology; part I: aerodynamic propulsive. *27th AIAA Applied Aerodynamics Conference*, AIAA, San Antonio TX, AIAA-2009-3942, 2009.

[23] Gaeta R J, Englar R J and Avera M. Development of pneumatic over-the-wing powered lift technology art II: aeroacoustics. *27th AIAA Applied Aerodynamics Conference,* AIAA, San Antonio TX, AIAA-2009-3941, 2009.

[24] Macpherson L. The wet look that lasts: Imron--the choice of truck manufacturers and commercial refinishers for 32 years. *Painting and Coating Industry*, 2005.

[25] Monson D J, Mateer G G and Menter F R. Boundary-layer transition and global skin friction measurements. *SAE 932550*, Society of Automotive Engineers, Costa Mesa CA, 1993.

[26] Zilliac - G G. The fringe-imaging skin friction technique PC application user's manual. *NASA Technical Memorandum 1999-208794*, NASA Ames Research Center, Moffett Field CA, 1999.

[27] Naughton - J W, and Sheplak M. Modern developments in shear-stress measurement. *Progress in Aerospace Sciences*, Vol. 38, No. 1, pp. 515-570, 2002.

[28] Zilliac -G G. Further Developments of the fringe-imaging skin friction technique. *NASA Technical Memorandum 110425*, NASA Ames Research Center, Moffett Field CA, 1996.

[29] Driver - D M, and Drake A. Skin-friction measurements using oil-film interferometry in NASA's 11-foot transonic wind tunnel. *AIAA Journal*, Vol. 46, No. 10, pp. 2401-2407, 2008.

[30] Ehrmann - R, Paciano E, and Jameson K K. Application of the FISF technique to a blended, 2-foot wing section. *28th AIAA Applied Aerodynamics Conference*, Chicago Il, AIAA-2010-4830, 2010.

[31] Hwang D, Fralick G C, Martin L C, Wrbanek J D, and Blaha C A. An innovative flow measuring device-thermocouple boundary layer rake. *NASA/TM—2001-211161*, 2001.

[32] Kendall J M. -Boundary layer receptivity to weak freestream turbulence. *NASA/CP—2007-214667*, March 2007.

[33] Fralick G, -Wrbanek J D, Hwang D, and Turso J. Sensors for using times of flight to measure flow velocities. *NASA Technical Briefs*, LEW-17944-1, 2006.

[34] The -Mathworks Inc., Natick, MA, MATLAB, 7th ed., 2008.

[35] Ehrmann - R, and Jameson K K. Design and fabrication of a micro flow measurement device. *40th Fluid Dynamics Conference and Exhibit*, Chicago Il, AIAA-2010-4622, 2010.

Copyright Statement